Proceedings of the ASME 2024
Pressure Vessels & Piping Conference
PVP2024
July 28 – August 2, 2024, Bellevue, Washington, USA

PVP2024-122529

TECHNICAL BASIS FOR FATIGUE CRACK GROWTH RULES IN GASEOUS HYDROGEN FOR ASME B31.12 CODE CASE 220 AND FOR REVISION OF ASME VIII-3 CODE CASE 2938-1

Chris San Marchi[1], Joseph A. Ronevich[1], Paolo Bortot[2], Matteo Ortolani[2], Kang Xu[3], Mahendra Rana[4]

[1]Sandia National Laboratories, Livermore CA, USA
[2]Tenaris, Dalmine, Italy
[3]Linde Inc, Tonawanda NY, USA
[4]consultant, Niantic CT, USA

ABSTRACT

Emerging hydrogen technologies span a diverse range of operating environments. High-pressure storage for mobility applications has become commonplace up to about 1,000 bar, whereas transmission of gaseous hydrogen can occur at hydrogen partial pressure of a few bar when blended into natural gas. In the former case, cascade storage is utilized to manage hydrogen-assisted fatigue and the Boiler and Pressure Vessel Code, Section VIII, Division 3 includes fatigue design curves for fracture mechanics design of hydrogen vessels at pressure of 1,030 bar (using a Paris Law formulation). Recent research on hydrogen-assisted fatigue crack growth has shown that a diverse range of ferritic steels show similar fatigue crack growth behavior in gaseous hydrogen environments, including low-carbon steels (e.g., pipeline steels) as well as quench and tempered Cr-Mo and Ni-Cr-Mo pressure vessel steels with tensile strength less than 915 MPa. However, measured fatigue crack growth is sensitive to hydrogen partial pressure and fatigue crack growth can be accelerated in hydrogen at pressure as low as 1 bar. The effect of hydrogen partial pressure from 1 to 1,000 bar can be quantified through a simple semi-empirical correction factor to the fatigue crack growth design curves. This paper documents the technical basis for the pressure-sensitive fatigue crack growth rules for gaseous hydrogen service in ASME B31.12 Code Case 220 and for revision of ASME VIII-3 Code Case 2938-1, including the range of applicability of these fatigue design curves in terms of environmental, materials and mechanics variables.

Keywords: Hydrogen Testing, Fatigue, High-Pressure

NOMENCLATURE

b	constant in gaseous equation of state for hydrogen
C	constant in fatigue crack growth equation (also C_{low} and C_{high})
C_H	constant in $f(R_k)$ (also $C_{H,low}$ and $C_{H,high}$)
da/dN	fatigue crack growth rate
$g(P)$	function representing pressure dependence in hydrogen-assisted fatigue crack growth
f	fugacity
f_H	fugacity of hydrogen (e.g in a gas mixture)
f_o	reference fugacity
$f(R_k)$	function representing dependence of fatigue crack growth on R_k
K_{max}	maximum stress intensity factor
ΔK	cyclic stress intensity factor range
ΔK_a	value of ΔK at which fatigue crack growth in air and hydrogen are equivalent
ΔK_c	value of ΔK at which hydrogen-assisted fatigue crack growth in the high-ΔK and low-ΔK regimes are equivalent
m	constant, exponent (also m_{low} and m_{high})
P	pressure
P_H	hydrogen partial pressure
P_t	total pressure
R	universal gas constant
R_k	stress intensity ratio
S	hydrogen solubility
S_y	yield strength
T	absolute temperature
V_m	molar volume
$[H]$	hydrogen concentration

1. INTRODUCTION

Hydrogen-assisted fatigue crack growth is an important design consideration for highly stressed components that experience pressure fluctuations in hydrogen service, such as high-pressure storage vessels and transmission pipelines. The ASME Boiler and Pressure Vessel Code, Section VIII, Division 3 (BPVC VIII-3) includes design requirements for high-pressure hydrogen storage vessels in Article KD-10. BPVC Code Case 2938-1 (CC2938-1) provides a fatigue crack growth rate formulation that can be used for fatigue design with hydrogen pressure up to 103 MPa, thus eliminating the necessity of fatigue testing in gaseous hydrogen at these high pressures. The hydrogen-assisted fatigue design curves in CC2938-1 were developed based on measurements of fatigue crack growth for SA-372 Grade J steels (quench and tempered Cr-Mo steels) and SA-723 Class 1 steels (quench and tempered Ni-Cr-Mo steels) (see Ref. [1] and references therein). CC2938-1 limits the use of these fatigue design curves to steels with tensile strength up to 915 MPa, because the fracture resistance declines rapidly with greater tensile strength, affecting the fatigue crack growth response. More recent research has explored microstructural variations and shown engineering-relevant microstructures do not substantially change the hydrogen-assisted fracture trends of conventional quenched and tempered steels [2]. Hydrogen-assisted fatigue and fracture of pressure vessel steels have been shown to depend on the hydrogen partial pressure [3], whereas CC2938-1 is based on an upper bound pressure of 103 MPa, which can be overly conservative when applied to lower pressure conditions. It is important to recognize, however, that at high ΔK, hydrogen-assisted fatigue crack growth is insensitive to pressure for both pressure vessel steels [3] and pipeline steels (this paper).

The technical basis of CC2938-1 [1] noted (but did not implement in the CC) that a simple empirical correction can be used to account for pressure and this pressure-dependent formulation applies to carbon and low alloys steels, such as conventional linepipe steels based on API 5L, and their welds. The pressure-dependent fatigue design curves have been used in several studies as a benchmark for comparison and upper bound of fatigue crack growth [3-9]. These studies emphasize that the hydrogen-assisted fatigue crack growth response of a broad range of steel grades and microstructures is consistent for the same environmental conditions and can be bounded by pressure-dependent fatigue design curves that originated in CC2938-1.

This paper summarizes the assumptions and development of the fatigue design curves in CC2938-1 and describes the pressure dependence and its formulation, thus providing the technical basis for the recently adopted ASME B31 Code Case 220 and the proposed revision to Code Case 2938-1.

2. FATIGUE DESIGN CURVES: BPVC VIII.3 CC2938-1

As hydrogen infrastructure for hydrogen fuel cell electric vehicles (FCEVs) was deployed, fatigue crack growth data in high-pressure hydrogen were needed for the design of storage vessels at hydrogen refueling stations (HRS). Commercial, passenger FCEVs store hydrogen fuel onboard the vehicle at pressure of 70 MPa, thus fuel storage at the HRS is significantly higher. This industry need drove the development of codes and standards (such as BPVC VIII-3 Article KD-10), as well as the development of capabilities to measure fatigue crack growth in gaseous hydrogen at pressure greater than 100 MPa [10-13].

A variety of quenched and tempered pressure vessel steels display similar fatigue crack growth rates (FCGR) when tested in gaseous hydrogen (GH2) at pressure of ~100 MPa [1, 3, 14], including several varieties of Cr-Mo and Ni-Cr-Mo steels certified to either the SA-372 or SA-723 standard. The fatigue response of these steels is characterized by two regions, generally referred to as the low ΔK and high ΔK regimes, and each of which can be represented by a power law, but with different exponents. Moreover, curve fits of the fatigue crack growth rates at different load ratios were found to have a similar slope in these two regions respectively, although the FCGR were dependent on the applied stress intensity ratio, R_k. These characteristics allow the construction of power laws representing the data, where the effect of the stress intensity ratio can be entirely captured by the pre-exponential factor, such that the exponent m is independent of R_k. The resulting power laws can thus be expressed, in general form, as

$$\frac{da}{dN} = C\, f(R_k)\, \Delta K^m$$

where da/dN is the FCGR, C and m are constants, $f(R_k)$ is a function of the stress intensity ratio R_k, ΔK is the cyclic stress intensity factor range. Based on the data available at the time of development of the initial fatigue design curves, the exponent m was evaluated to be 3.66 and 6.5 in the low ΔK and high ΔK regimes, respectively. The FCGR data in each regime was then curve fit again, after fixing the exponents, to determine the product $C\, f(R_k)$. This term was then curve fit as a function of R_k to determine a simple functional form that represented the data in each regime, respectively. This functional form was empirically defined as:

$$f(R_k) = \left[\frac{1 + C_H R_k}{1 - R_k}\right]$$

where C_H is a constant determined from the curve fitting. Using m and $f(R_k)$, the constant C was determined to establish upper bound on the experimental data for FCGR in each regime. The resulting constants are given in Table 1.

The transition between the fatigue design curves at low and high ΔK is established mathematically when da/dN resulting from the two power law formulations are equal for a given value of R_k. That is, the value of the stress intensity factor range at which these two power laws are equivalent (denoted ΔK_c) can be expressed in closed form as:

$$log(\Delta K_c) = \frac{C_{low}\left[\frac{1 + C_{H,low} R_k}{1 - R_k}\right]}{C_{high}\left[\frac{1 + C_{H,high} R_k}{1 - R_k}\right]} \Big/ \left(m_{high} - m_{low}\right)$$

Since ΔK_c is only a function of R_k, it can be conveniently approximated with a polynomial fit as

$$\Delta K_C = 8.475 + 4.062 R_K + 1.696 {R_K}^2$$

where ΔK_c is in units of MPa m$^{1/2}$.

It is important to recognize that FCGR relationships are not unbounded; a fact that is often not articulated along with published relationships. As the maximum stress intensity factor (K_{max}) in fatigue approaches the fracture toughness of the material, simple power laws no longer capture the fatigue response as the crack extension process transitions from fatigue to fracture. This characteristic was noted in developing the hydrogen-assisted fatigue crack growth curves for pressure vessel steels [14]. Evaluation of pressure vessel steels in high-pressure GH2 reveals low fracture resistance when tensile strength exceeds about 900 MPa; specifically, the fracture resistance in GH2 at pressure of 106 MPa is less than 40 MPa m$^{1/2}$ when the tensile strength is greater than 915 MPa. Therefore, CC2938-1 limits application of the fatigue design curves to $K_{max} < 40$ MPa m$^{1/2}$ and tensile strength < 915 MPa. An example of FCGR data for several pressure vessel steels is shown in Figure 1, along with the fatigue design curve (at pressure of 106 MPa) and the deviation of high-strength steels from the hydrogen-assisted fatigue design curves.

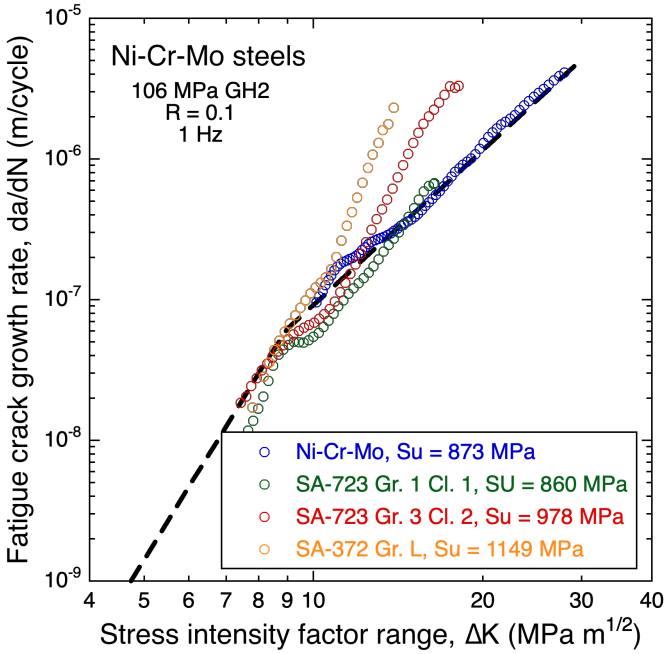

Figure 1. Fatigue crack growth curves for several pressure vessel steels, measured in gaseous hydrogen at pressure of 106 MPa. The dashed line represents fatigue design curve from CC2938-1. For the steels with tensile strength (Su) greater than 915 MPa, the FCGR is not bounded by the fatigue design curves for large ΔK.

3. PRESSURE EFFECTS

At the time of constructing the original fatigue design curves, it was recognized that the FCGR in GH2 depends on the hydrogen partial pressure [1]. Therefore, a simple pressure-dependent term was proposed of the form:

$$\frac{da}{dN} = C\, f(R_k)\, \Delta K^m f(P)$$

where $f(P)$ can have different forms depending on the conditions of interest. For example, it was recognized that hydrogen-assisted fatigue crack growth is insensitive to pressure in the high ΔK regime for both pipeline and pressure vessel steels [1, 4]. Therefore, $f(P) = 1$ for fatigue in the high-ΔK regime ($\Delta K > \Delta K_c$). Conversely, various forms of $f(P)$ in the low-ΔK regime are possible, therefore we use $g(P)$ to represent the general form of the pressure dependence in the low-ΔK regime. In other words:

$$\begin{aligned} &\text{for } \Delta K \le \Delta K_c && f(P) = g(P) \\ &\text{for } \Delta K > \Delta K_c && f(P) = 1 \end{aligned}$$

where $g(P)$ depends on several factors and will be defined in terms of thermodynamic considerations in the following.

Due to the exponential nature of the FCGR and the challenges testing in GH2, it is difficult to quantitatively characterize the effect of pressure in a general form from data alone. However, thermodynamically the amount of lattice hydrogen in a metal in equilibrium with GH2 is related to the square root of the thermodynamic pressure [15]. This is often expressed as the general form of Sieverts' Law:

$$[H] = S f^{1/2}$$

where $[H]$ is the equilibrium lattice hydrogen concentration in the steel, f is the thermodynamic pressure or fugacity (which reduces to the pressure for an ideal gas), and S is the hydrogen solubility. If hydrogen-assisted fatigue in the low-ΔK regime is assumed to be proportional to the lattice hydrogen concentration in the steel, then $da/dN \propto f^{1/2}$. As described in the previous section, FCGR design curves have been established for quenched and tempered pressure vessel steels (within defined bounds on the material) at pressure of 106 MPa [1]; this pressure is defined as the reference pressure. With the above assumption, FCGR in the low-ΔK regime can be determined at any hydrogen partial pressure in relationship to this reference pressure. In other words, the FCGR design curve for low ΔK from CC2938-1 can be scaled by a simple factor of $(f/f_o)^{1/2}$, where f is the fugacity at the pressure of interest and f_o is the fugacity at the reference pressure of 106 MPa [1]. The empirical pressure dependence in the low-ΔK regime is then formulated as

$$g(P) = (f/f_o)^{1/2}.$$

Additionally, since ASME BPVC VIII-3 gives a single fatigue crack growth relationship for carbon and low-alloy steels ($S_y \le$

620 MPa, Table D-500, 2019 edition) in air, one might expect the hydrogen-assisted fatigue design curves to be appropriate for carbon steels as well as for low-alloy pressure vessel steels. Indeed, the pressure-dependent form of the hydrogen-assisted fatigue design curve was proposed in Ref. [1] and demonstrated for a variety of carbon (pipeline) steels at lower pressures [5].

The formulations described above have been validated against a few dozen carbon and low-alloy steels at hydrogen partial pressure from about 0.1 to 106 MPa [3-9, 14]. The tested carbon steels have typically been evaluated in the lower pressure regime (less than about 20 MPa), whereas the low-alloy steels have been mostly evaluated at higher pressure (about 50 to 100 MPa). However, some high-strength carbon steels have been evaluated at nominally 100 MPa [16], and low-alloy steels as low as about 20 MPa [3, 17]. Several additional examples are shown in Figures 2 to 4.

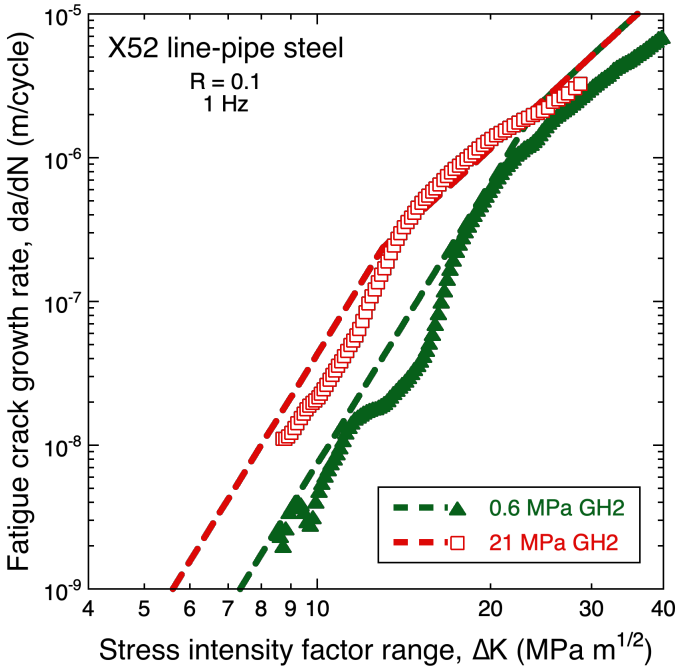

Figure 2. Fatigue crack growth of an X52 grade pipeline steel in pure gaseous hydrogen and in nitrogen with 3% hydrogen. For both conditions the total pressure was 21 MPa. In the low-ΔK regime, fatigue clearly depends on the partial pressure of hydrogen; whereas in the high-ΔK regime, the fatigue crack growth rates for the two conditions converge to a pressure-independent response. The dashed lines represent the fatigue design curves for these conditions.

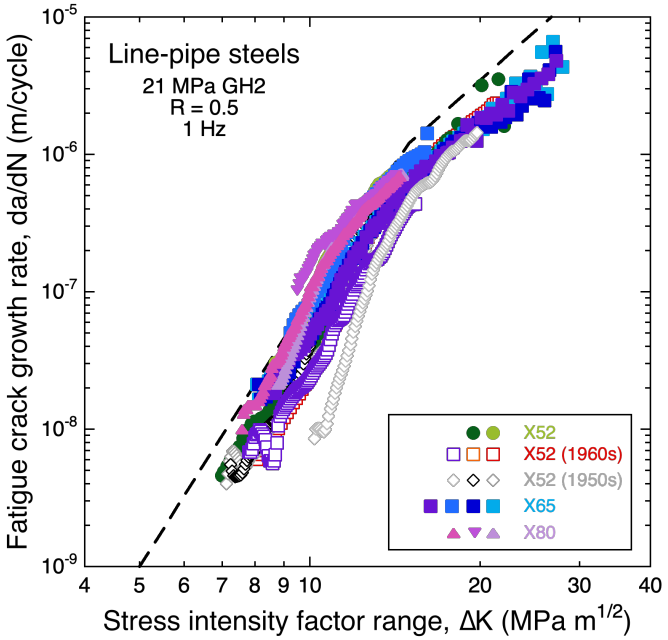

Figure 3. Fatigue crack growth for a range of vintage and modern pipeline steels in gaseous hydrogen at pressure of 21 MPa and $R = 0.5$. The dashed line represents the fatigue design curve for this testing condition.

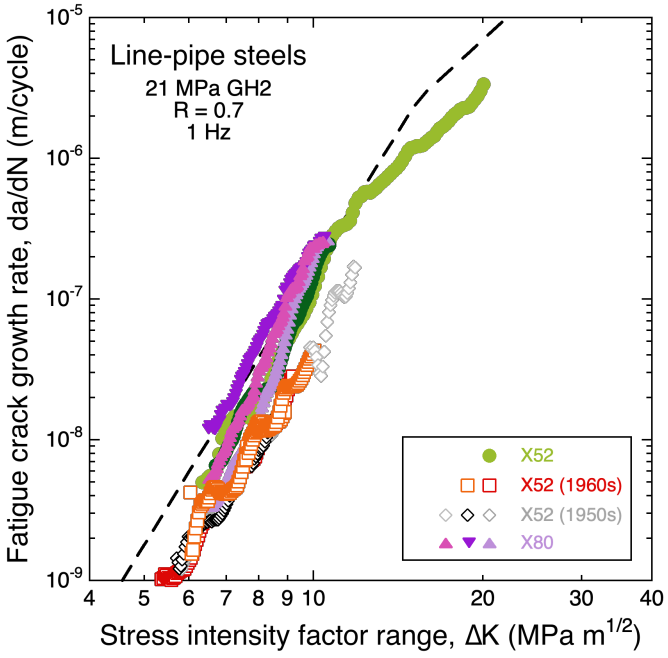

Figure 4. Fatigue crack growth for a range of vintage and modern pipeline steels in gaseous hydrogen at pressure of 21 MPa and $R = 0.7$. The dashed line represents the fatigue design curve for this testing condition.

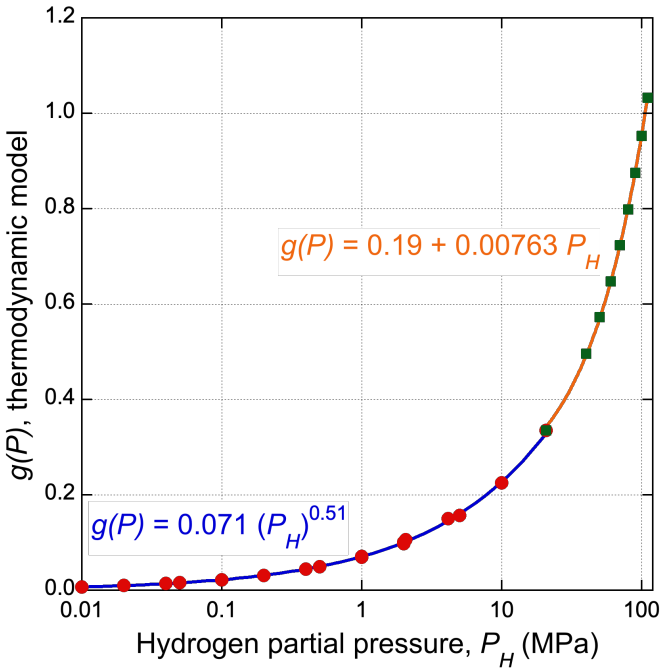

Figure 5. Curve fits of the thermodynamic model for $g(P)$ as a function of hydrogen partial pressure. The symbols represent the thermodynamic model; the different colors represent low pressure (P_H < 20 MPa) and high pressure (P_H between 20 and 120 MPa), respectively.

4. PRESSURE DEPENDENCE: *g(P)* AND FUGACTIY

In this section, the general pressure dependent term $g(P)$ is derived for thermodynamic principles and an approximation for $g(P)$ is proposed as a function of only the hydrogen partial pressure. In simple terms, fugacity is the pressure of an ideal gas that performs equivalently to the real (non-ideal) gas. The fugacity is not a measurable pressure, rather fugacity is a quantity that represents the thermodynamic character of the gas in real-world conditions, also called the thermodynamic pressure.

The fugacity is determined from the equation of state (EOS) that describes the gas behavior. There are numerous forms of the EOS for hydrogen (and other gases), the simplest being the ideal gas law. Perhaps the simplest non-ideal gas EOS has the form

$$V_m = \frac{RT}{P} + b$$

and is often referred to as the Abel-Noble EOS, where V_m is the molar volume, P is pressure, R is the universal gas constant, T is the absolute temperature and b is the co-volume constant (=15.84 cm^3/mol for hydrogen [15]). This EOS was optimized for pressure and temperature ranges of engineering significance, as described in Ref [15]. Using this simple EOS, an analytical expression for the fugacity can be derived [4, 15] as

$$\frac{f}{P} = \exp\left(\frac{Pb}{RT}\right)$$

In the limit of an ideal gas ($b \to 0$), this expression reduces to $f = P$, as expected. For a mixed or blended gas, the fugacity of hydrogen depends on both the partial pressure of hydrogen and the total pressure.

The influence of the total pressure may be relatively small in most cases (a few percent), but it can be incorporated analytically as described elsewhere [4, 18]. Assuming that the gas species in the mixture do not interact (i.e., an ideal mixture), the fugacity of any phase is proportional to its volume fraction. Therefore, the fugacity of hydrogen in a mixture (f_H) can be expressed as a function of the partial pressure of hydrogen (P_H) and the total pressure (P_t) as

$$\frac{f_H}{P_H} = \exp\left(\frac{P_t b}{RT}\right)$$

As mentioned above, the fatigue design curves were developed for (pure) hydrogen at a pressure of 106 MPa, which we refer to as the reference pressure (P_o) associated with the reference fugacity (f_o). Combining these relationships for the general case of hydrogen in a gas mixture, the pressure dependence can be expressed as a relatively simple analytical expression:

$$g(P) = \left(\frac{f_H}{f_o}\right)^{1/2} = \left[\left(\frac{P_H}{P_o}\right)\exp\left(\frac{b}{RT}(P_t - P_o)\right)\right]^{1/2}$$

where P_H is the partial pressure of hydrogen, P_t is the total pressure, and P_o is the reference pressure (=106 MPa). We must emphasize that $g(P)$ is defined in terms of the partial pressure of hydrogen (P_H or, more precisely, f_H). The expression for $g(P)$ can be reduced to a simple function of the hydrogen partial pressure through curve fitting; however, a reduced order expression cannot capture the entire range of P_H up to 100 MPa. Therefore, as an alternative to the full analytical expression, reduced-order expressions were developed for room temperature as

for P_H < 20 MPa:	$g(P) = 0.071\ (P_H)^{0.51}$
for 20 ≤ P_H ≤ 120 MPa:	$g(P) = 0.19 + 0.00763 P_H$

Units are important and these relationships assume pressure unit of 'MPa'; these expressions can easily be converted to U.S. customary units or other units. The low-pressure relationship was fit to the full expression for total pressure from 0.1 to 20.7 MPa and volume fraction of hydrogen of 0.1, 0.2 and 1. This range of conditions emphasize low partial pressure of hydrogen in gas mixtures, which show the largest deviation from the pure hydrogen case (the latter is also included, i.e., volume fraction of 1). The high-pressure range was fit only for pure hydrogen between 40 and 110 MPa. In this pressure range, blending hydrogen is less technologically relevant and the difference in fugacity between pure hydrogen and gas mixture (with total pressure not exceeding 120 MPa) becomes small. The values of $g(P)$ from the full expression and the resulting curve

fits are shown in Figure 5. As evident in this figure, extrapolation of the high-pressure, reduced-order relationship to 20 MPa is a conservative estimate of $g(P)$ compared to the low-pressure relationship (and still within <5%). Additionally, the curve fit for the high-pressure range was chosen to emphasize the technologically relevant pressure range of 40 to 110 MPa; extrapolation to the bounds of 20 and 120 MPa is reasonable based on the functional form of $g(P)$ and should be evident from the figure. High-pressure, low-concentration blends (such as, $P_t > 50$ MPa, $P_H < 20$ MPa) may need to be considered separately.

5. FATIGUE DESIGN CURVES: B31.12 CC220

As noted above, the fatigue design curves from CC2938-1 for a pressure of 106 MPa are appropriate for carbon steels, but the predicted FCGR will be conservative at the lower pressure in pipelines. Implementing the pressure dependence, as described above, will remove conservativism but will impact the transition between the low-ΔK and high-ΔK regimes. As described in Section 3, a pressure-dependent formulation was proposed, whereas Section 4 quantitatively describes the pressure-dependent term for the low-ΔK regime: $g(P)$. The addition of pressure dependence affects the transition between the low-ΔK and high-ΔK regimes and must be considered.

Quantification of the transition (ΔK_c) is accomplished in the same way as described in Section 2, except the revised pressure-dependent relationship is used. Noting that $f(P) = 1$ in the high ΔK regime, ΔK_c can be expressed in closed form as:

$$log(\Delta K_c) = \frac{\dfrac{C_{low}\left[\dfrac{1 + C_{H,low}R_k}{1 - R_k}\right] g(P)}{C_{high}\left[\dfrac{1 + C_{H,high}R_k}{1 - R_k}\right]}}{(m_{high} - m_{low})}$$

where $g(P)$ describes the pressure dependence in the low-ΔK regime. Since the adopted formulation of *da/dN* includes independent terms for dependency of R_k and P_H (the latter through the $g(P)$ term), the dependence of ΔK_c on these variables should also be separable. To establish the dependence of ΔK_c on hydrogen partial pressure, ΔK_c was determined for values of R_k between 0 and 0.9 at 0.1 intervals as well as at R_k = 0.05 and 0.95 (to ensure adequate emphasis of the endpoints). Power-law fits with pressure at each R_k revealed an exponent of approximately -0.18 for all values of R_k (i.e., $\Delta K_c \propto P^{-0.18}$ for all R_k between 0 and 0.95). To determine the R_k dependence, a polynomial was fit to the quantity $\Delta K_c / {P_H}^{-0.18}$ for pressure between 0.1 and 20.7 MPa. The simplified expression for ΔK_c is then

$$\Delta K_c = \left(21.66 + 10R_k - 3.7{R_k}^2\right){P_H}^{-0.18}$$

In addition to the transition between the low- and high-ΔK regimes, we must also consider the baseline FCGR in air. Extrapolation of the fatigue design curves to low hydrogen partial pressure can predict *da/dN* in hydrogen that is less than in air. While measurements of FCGR at low ΔK in hydrogen are relatively limited, there is information in the literature showing the FCGR at low rates in GH2 does not necessarily extend below the FCGR in air. In short, a second transition must be established where FCGR in air is equivalent to the FCGR in hydrogen; we identify this transition as ΔK_a. An analogous process can be followed to develop a relationship for ΔK_a as a function of R_k and P_H. The formulation will depend on the *da/dN*-ΔK relationship chosen for air. For ASME B31.12 CC220, the FCGR relationship for air from the BPVC VIII-3 was selected, which is expressed as

$$da/dN_{air} = 3.8\,x10^{-12}\left(\frac{2.88}{2.88 - R_k}\right)^{3.07}\Delta K^{3.07}$$

where units are m/cycle and MPa m$^{1/2}$ for *da/dN* and ΔK respectively. The resulting relationship for ΔK_a as a function of R_k and P_H (<20 MPa) is

$$\Delta K_a = \left(8.6 - 3.0R_k + 7.9{R_k}^2 - 9.4{R_k}^3\right){P_H}^{-0.15}$$

Consequently, CC220 establishes three zones of FCGR:
(1) fatigue in air for $\Delta K < \Delta K_a$, equivalent in air and hydrogen
(2) low-ΔK hydrogen-assisted fatigue for $\Delta K_a \leq \Delta K \leq \Delta K_c$
(3) high-ΔK hydrogen-assisted fatigue for $\Delta K > \Delta K_c$

These three regimes are shown in Figure 6 and the relevant *da/dN* relationships are summarized in Table 2. Since the application of B31.12 part PL is limited to maximum operating pressure of 20 MPa, $g(P)$ in CC220 is only specified for the low-pressure range ($P_H < 20$ MPa).

It should be noted that CC2938-1 limits the applicability of the design curves to $K_{max} < 40$ MPa m$^{1/2}$ and tensile strength < 915 MPa, whereas there is no explicit limit on K_{max} in CC220 for pipeline steels. These limits remain generally appropriate for pipeline steels but will be conservative in some cases. Some vintage pipeline steels display relatively low fracture resistance, thus K_{max} of 40 MPa m$^{1/2}$ is an appropriate bound (as described above the fracture resistance is an important metric for applicability of the fatigue design curves). The strength of pipeline steels is general lower than low-alloy steels used in pressure vessels; additionally, the hydrogen pressure in pipeline applications is relatively low (P_H < 20 MPa) compared to pressure vessels (up to 103MPa in CC2938). For both reasons, the fracture resistance of high-quality pipeline steels can be significantly greater than 40 MPa m$^{1/2}$, suggesting that the design curves may be appropriate for higher K_{max} commensurate with the fracture resistance of the steel in the applicable environment.

It is worth remarking that whereas CC 2938-1 concerns integrally forged vessels and parts not intended to be welded, CC 220 addresses FCGR in base metal and weldments. Ronevich et al. has shown that welds perform similarly to base metals for linepipe steels when the influence of residual stress is removed from the FCGR data [19-23]. In fact, because of stress concentrations at welds, most of fatigue issues are likely to occur

in pipeline welds or HAZ rather than in base metal. When FCGR is calculated for these portions, the residual stress state must be considered, since it impacts the stress intensity ratio R_k. Thus, CC 220 provides guidance to include a term to account for weld residual stresses in stress intensity factor calculations.

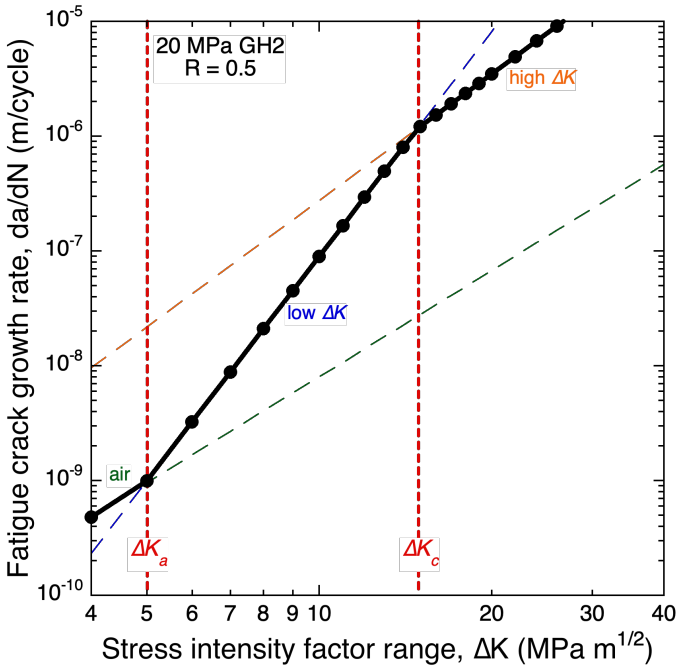

Figure 6. Fatigue design curves in black, showing the three regimes of crack growth in hydrogen: (1) fatigue crack growth rate in air for $\Delta K < \Delta K_a$; (2) the low-ΔK (and pressure dependent) regime between ΔK_a and ΔK_c; (3) the high-ΔK regime (pressure independent) for $\Delta K > \Delta K_c$.

6. REVISION OF CC2938-1

As described above, CC2938-1 provides upper bound fatigue design curves for pressure of 103 MPa (the relationships were determined based on measurement in GH2 at pressure of 106 MPa, although the code case limits application to 103 MPa). As described in Refs. [3, 17], testing in lower pressure GH2 results in lower measured FCGR. The design curves for low-alloy steels (such as SA-372 and SA-723) can be adjusted for conditions of lower pressure hydrogen in the same way as discussed in previous sections. Additionally, CC220 only considered pressure less than about 20 MPa. For higher pressure, the relationships for carbon steels require refinement for the change of the functional form of $g(P)$. Whereas ΔK_c does not depend on the material, the formulations described here depend on the pressure range of interest (due to the two forms of the $g(P)$ relationship for pressure less than and greater than 20 MPa respectively), thus two relationships for ΔK_c are needed to describe the full pressure range and are shown in Table 3a. In contrast, ΔK_a depends on the *da/dN*-ΔK relationship in air. The ASME BPVC VIII-3 provides different forms of FCGR in air for carbon and low-alloy steels with yield strength ≤ 620 MPa (as used for CC220) and for high-strength, low-alloy steels with yield strength > 620 MPa. For each of these material classes, there are two forms for ΔK_a representing the two different pressure regimes (i.e., different formulations for $g(P)$). Therefore, for these conditions, four relationships for ΔK_a are needed for a complete description of the fatigue of carbon and low-alloy steels at pressure between 0.1 and 103 MPa. The ΔK_a relationships are summarized in Table 3b. Collectively, these tables (Tables 2, 3a & 3b) represent a complete set of fatigue design curves that can be adopted in CC2938 to include both carbon and low-alloy steels with tensile strength < 915 MPa for hydrogen partial pressure in range of 0.1 to 103 MPa, and applicable to R_k from 0 to 0.95 when K_{max} < 40 MPa m$^{1/2}$.

Presently, CC 2938 revision to incorporate the full pressure dependent formulations for hydrogen-assisted FCGR is under discussion in ASME BPVC Section VIII Committees under record number 23-2639.

7. SUMMARY

Extensive fatigue crack growth testing in GH2 has shown consistency in hydrogen-assisted fatigue crack growth for a wide range of carbon and low-alloy steels (reflective of the common FCGR for these materials in air, as described in BPVC VIII-3). ASME BPVC CC 2938-1 provided hydrogen-assisted fatigue design curves for pressure vessel steels in high-pressure gaseous hydrogen, which represent the upper bound FCGR at hydrogen pressure of 103 MPa.

ASME B31.12 CC220 adapted these design curves for pipeline steels for hydrogen partial pressure ≤ 20 MPa, by implementing a pressure-dependent term and noting the transition (ΔK_a) between fatigue in air and in hydrogen at low ΔK (to prevent extrapolation of hydrogen-assisted design curves to FCGR less than in air). CC220 also includes a term to account for the effect of residual stresses to enable these curves to be applied to base metal, heat affected zone and weld metal.

This paper describes the technical basis for B31.12 CC 220 and for revision of BPVC VIII-3 CC 2938-1, advancing hydrogen-assisted fatigue crack growth curves for use with both carbon and low-alloys steels for hydrogen partial pressure from 0.1 to 103 MPa.

ACKNOWLEDGEMENTS

This material is based upon work supported by the U.S. Department of Energy's Office of Energy Efficiency and Renewable Energy (EERE) under the Hydrogen and Fuel Cell Technologies Office (HFTO) Safety Codes and Standards sub-program, under the direction of Laura Hill. This article has been authored by an employee of National Technology & Engineering Solutions of Sandia, LLC under Contract No. DE-NA0003525 with the U.S. Department of Energy (DOE). The employee owns all right, title and interest in and to the article and is solely responsible for its contents. The United States Government retains and the publisher, by accepting the article for publication, acknowledges that the United States Government retains a non-exclusive, paid-up, irrevocable, world-wide license to publish or reproduce the published form of this article or allow others to do so, for United States Government purposes. The DOE will provide public access to these results of federally

sponsored research in accordance with the DOE Public Access Plan https://www.energy.gov/downloads/doe-public-access-plan. This paper describes objective technical results and analysis. Any subjective views or opinions that might be expressed in the paper do not necessarily represent the views of the U.S. Department of Energy or the United States Government.

REFERENCES

[1] C San Marchi, J Ronevich, P Bortot, Y Wada, J Felbaum, and M Rana. Technical basis for master curve for fatigue crack growth of ferritic steels in high-pressure gaseous hydorgen in ASME Section VIII-3 code (PVP2019-93907). ASME Pressure Vessels and Piping Division Conference, San Antonio TX, 14-19 July 2019.

[2] J Ronevich, B Kagay, C San Marchi, Y Wang, Z Feng, and W Yanli. Investigating the role of ferritic steel microstructure and strength in fracture resistance in high-pressure hydrogen gas (PVP2022-83915). ASME Pressure Vessels and Piping Division Conference, Las Vegas NV, 17-22 July 2022.

[3] P Bortot, M Ortolani, C San Marchi, and J Ronevich. Effect of hydrogen partial pressure on fatigue crack growth rates of low alloy, quench and tempered steels (PVP2023-106417). ASME Pressure Vessels and Piping Division Conference, Atlanta GA, 16-21 July 2023.

[4] JA Ronevich and C San Marchi. Materials compatibility concerns for hydrogen blended into natural gas (PVP2021-62045). ASME Pressure Vessels and Piping Division Conference, Virtual/Online, 13-15 July 2021.

[5] C San Marchi and J Ronevich. Fatigue and fracture of pipeline steels in high-pressure hydrogen gas (PVP2022-84757). ASME Pressure Vessels and Piping Division Conference, Las Vegas NV, 17-22 July 2022.

[6] M Agnani, JA Ronevich, J Parker, M Gagliano, S Potts, and C San Marchi. Fatigue and fracture behavior of vintage pipelines in gasoeus hydrogen environment (PVP2023-105622). ASME Pressure Vessels and Piping Division Conference, Atlanta GA, 16-21 July 2023.

[7] M Agnani, J Ronevich, and C San Marchi. Fatigue and fracture resistance of different line pipe grade steels in gaseous H2 environment. AMPP 2024 Annual Conference, New Orleans LA, 3-7 March 2024.

[8] M Agnani, J Ronevich, and C San Marchi. Comparison of fatigue and fracture behavior of welded and seamless pipe steel in gasoeus hydrogen. 3rd International Symposium on the Recent Developments in Plate Steels, Vail CO, 2-5 June 2024.

[9] M Agnani, J Ronevich, and C San Marchi. Comparison between fatigue and fracture behavior of pipeline steels in pure and blended hydrogen at different pressures (PVP2024-123477). ASME Pressure Vessels and Piping Conference, Bellevue WA, 29 July - 2 August 2024.

[10] BP Somerday, KA Nibur, and C San Marchi. Measurement of fatigue crack growth rates for steels in hdyrogen containment components. International Conference on Hydrogen Safety (ICHS), Ajaccio, Corsica, France, 16-18 September 2009.

[11] BP Somerday, C San Marchi, and K Nibur. Measurement of fatigue crack growth rates for SA-372 Gr. J steel in 100 MPa hydrogen gas folliwing article KD-10 (PVP2013-97455). ASME Pressure Vessels and Piping Division Conference, Paris, France, 14-18 July 2013.

[12] BP Somerday, P Bortot, and J Felbaum. Optimizing measurement of fatigue crack growth relationships for Cr-Mo pressure vessl steels in hydrogen gas (PVP2015-45424). ASME Pressure Vessels and Piping Division Conference, Boston MA, 19-23 July 2015.

[13] BP Somerday, JA Campbell, KL Lee, JA Ronevich, and C San Marchi. Enhancing safety of hydrogen containment components through materials testing under in-service conditions. *Int J Hydrogen Energy* 42 (2017) pp. 7314-7321. https://doi.org/10.1016/j.ijhydene.2016.04.189

[14] C San Marchi, P Bortot, Y Wada, and JA Ronevich. Fatigue and fracture of high-hardenability steels for thick-walled hydrogen pressure vessels. International Conference on Hydrogen Safety (ICHS), Hamburg, Germany, 11-13 September 2017.

[15] C San Marchi, BP Somerday, and SL Robinson. Permeability, Solubility and Diffusivity of Hydrogen Isotopes in Stainless Steels at High Gas Pressure. *Int J Hydrogen Energy* 32 (2007) pp. 100-116. https:/doi.org/10.1016/j.ijhydene.2006.05.008

[16] Y Wang, Z Feng, Y Wang, J Ronevich, M Agnani, and C San Marchi. Microstructure and mechanical performance of X120 linepipe steel in high-pressure hydrogen gas (PVP2024-123383). ASME Pressure Vessels and Piping Conference, Bellevue WA, 29 July - 2 August 2024.

[17] P Bortot, M Ortolani, M Bellingardi, C San Marchi, and J Ronevich. Investigating fatigue crack growth rate of ferritic steels in high pressure hydrogen gas. AMPP 2024 Annual Conference, New Orleans LA, 3-7 March 2024.

[18] C San Marchi and BP Somerday. Thermodynamics of Gaseous Hydrogen and Hydrogen Transport in Metals (1098-HH08-01). *Mater Res Soc Symp Proc Vol 1098*, MRS 2008 Spring Meeting, San Francisco CA, 24-28 March 2008.

[19] JA Ronevich and BP Somerday. Assessing gaseous hydrogen assisted fatigue crack growth susceptibility of pipeline steel weld fusion zones and heat affected zones. *Mater Perform Charac* 5 (2016) pp. 290-304.

[20] JA Ronevich and BP Somerday. Hydrogen effects on fatigue crack growth rates in pipeline steel welds (PVP2016-63669). ASME Pressure Vessels and Piping Division Conference, Vancouver, British Columbia, Canada, 17-21 July 2016.

[21] JA Ronevich, CR D'Elia, and MR Hill. Fatigue crack growth rates of X100 steel welds in high pressure hydrogen gas considering residual stress effects. *Eng Fract Mech* 194 (2018) pp. 42-51. https://doi.org/10.1016/j.engfracmech.2018.02.030

[22] JA Ronevich, EJ Song, Z Feng, Y Wang, CR D'Elia, and MR Hill. Fatigue crack growth rates in high pressure hydrogen gas for multiple X100 pipeline welds accounting for crack location and residual stress. *Eng Fract Mech* 228 (2020) p. 106846. https://doi.org/10.1016/j.engfracmech.2018.02.030

[23] JA Ronevich, EJ Song, BP Somerday, and C San Marchi. Hydrogen-assisted fracture resistance of pipeline welds in gaseous hydrogen. *Int J Hydrogen Energy* 46 (2021) pp. 7601-7614. https://doi.org/10.1016/j.ijhydene.2020.11.239

Table 1. Fatigue design curves for hydrogen as described in ASME BPVC CC2938-1. Hydrogen pressure for these relationships is 103 MPa.

ΔK range (MPa m$^{1/2}$)	C (m/cycle)	m	$f(R_k)$	C_H
$\Delta K < \Delta K_c$	3.5 x 10^{-14}	6.5	$\frac{1 + C_H R_k}{1 - R_k}$	0.43
$\Delta K_c \leq \Delta K \leq 40$	1.5 x 10^{-11}	3.66		2.0
$\frac{da}{dN} = C\, f(R_k)\, \Delta K^m$ $\Delta K_C = 8.475 + 4.062 R_K + 1.696 {R_K}^2$			Units: ΔK_c (MPa m$^{1/2}$) P_H (MPa)	

Table 2. Fatigue design curves for hydrogen as described in ASME B31 CC220 for carbon steels. Hydrogen partial pressure is limited to $P_H \leq 20.7$ MPa.

ΔK range (MPa m$^{1/2}$)	C (m/cycle)	m	$f(R_k)$	C_H	$f(P)$
$\Delta K < \Delta K_a$	3.8 x 10^{-12}	3.07	$\left(\frac{C_H}{C_H - R_k}\right)^m$	2.88	1.0
$\Delta K_a \leq \Delta K < \Delta K_c$	3.5 x 10^{-14}	6.5	$\frac{1 + C_H R_k}{1 - R_k}$	0.43	$g(P)$
$\Delta K \geq \Delta K_C$	1.5 x 10^{-11}	3.66		2.0	1.0
$\frac{da}{dN} = C\, f(R_k)\, \Delta K^m f(P)$ $g(P) = 0.071\, (P_H)^{0.51}$ $\Delta K_a = \left(8.6 - 3.0 R_k + 7.9 {R_k}^2 - 9.4 {R_k}^3\right) {P_H}^{-0.15}$ $\Delta K_c = \left(21.66 + 10 R_k - 3.7 {R_k}^2\right) {P_H}^{-0.18}$			Units: ΔK_a (MPa m$^{1/2}$) ΔK_c (MPa m$^{1/2}$) P_H (MPa)		

Table 3a. Pressure-dependent term and transition between low-ΔK and high-ΔK regimes: $g(P)$ and ΔK_c respectively both for carbon and low-alloy steels (tensile strength < 915 MPa).

P_H range (MPa)	$g(P)$	ΔK_c (MPa m$^{1/2}$)
0.1 to 20	$0.071\ (P_H)^{0.51}$	$\left(21.66 + 10R_k - 3.7{R_k}^2\right){P_H}^{-0.18}$
20 to 120	$0.19 + 0.00763P_H$	$\left(27.4 + 12.7R_k - 4.8{R_k}^2\right){P_H}^{-0.25}$
Formulation of *da/dN* is the same as Table 2, except $g(P)$ depends on pressure range.		

Table 3b. Transition between fatigue in air and hydrogen (ΔK_a) for carbon and low-alloy steels and for high-strength, low-alloy steels (in both cases, tensile strength < 915 MPa).

Material (S_y = yield strength)	da/dN_{air} (m/cycle)	P_H range (MPa)	ΔK_a (MPa m$^{1/2}$)
Carbon and low-alloy steels, $S_y \leq 620$ MPa	$3.8\ x10^{-12}\left(\frac{2.88}{2.88 - R_k}\right)^{3.07}\Delta K^{3.07}$	0.1 to 20	$\left(8.6 - 3.0R_k + 7.9{R_k}^2 - 9.4{R_k}^3\right){P_H}^{-0.15}$
		20 to 120	$\left(10.6 - 3.7R_k + 9.8{R_k}^2 - 11.7{R_k}^3\right){P_H}^{-0.21}$
High-strength, low-alloy steels $S_y > 620$ MPa	$3.64\ x10^{-12}(1 + 3.53R_k)\Delta K^{3.26}$	0.1 to 20	$\left(9.6 + 2.7R_k + 0{R_k}^2 - 7.8{R_k}^3\right){P_H}^{-0.16}$
		20 to 120	$\left(11.9 + 3.4R_k + 0{R_k}^2 - 9.6{R_k}^3\right){P_H}^{-0.22}$